GEOLOGY | THE GEOLOGICAL SOCIETY OF AMERICA®

https://doi.org/10.1130/G49214.1

Manuscript received 1 May 2021
Revised manuscript received 15 July 2021
Manuscript accepted 16 July 2021

Published online 30 August 2021

Contribution of orbital forcing and Deccan volcanism to global climatic and biotic changes across the Cretaceous-Paleogene boundary at Zumaia, Spain

Vicente Gilabert[1], Sietske J. Batenburg[2], Ignacio Arenillas[1] and José A. Arz[1]

[1]Departamento de Ciencias de la Tierra–Instituto Universitario de Investigación en Ciencias Ambientales de Aragón (IUCA), Universidad de Zaragoza, E-50009 Zaragoza, Spain

[2]Departament de Dinàmica de la Terra i de l'Oceà, Facultat de Ciències de la Terra, Universitat de Barcelona, 08028 Barcelona, Spain

ABSTRACT

Untangling the timing of the environmental effects of Deccan volcanism with respect to the Chicxulub impact is instrumental to fully assessing the contributions of both to climate change over the Cretaceous-Paleogene boundary (KPB) interval. Despite recent improvements in radiometric age calibrations, the accuracy of age constraints and correlations is insufficient to resolve the exact mechanisms leading to environmental and climate change in the 1 m.y. across the KPB. We present new high-resolution planktic foraminiferal, geochemical, and geophysical data from the Zumaia section (Spain), calibrated to an updated orbitally tuned age model. We provide a revised chronology for the major carbon isotope excursions (CIEs) and planktic foraminiferal events and test temporal relationships with different models of the eruptive phases of the Deccan Traps. Our data show that the major CIEs near the KPB, i.e., the late Maastrichtian warming event (66.25–66.10 Ma) and the Dan-C2 event (65.8–65.7 Ma), are synchronous with the last and the first 405 k.y. eccentricity maximum of the Maastrichtian and the Danian, respectively, and that the minor Lower C29n event (65.48–65.41 Ma) is well constrained to a short eccentricity maximum. Conversely, we obtained evidence of abrupt environmental change likely related to Deccan volcanism at ca. 65.9 Ma, based on a bloom of opportunistic triserial guembelitriids (*Chiloguembelitria*). The orbital, isotopic, and paleobiological temporal relationships with Deccan volcanism established here provide new insights into the role of Deccan volcanism in climate and environmental change in the 1 m.y. across the KPB.

INTRODUCTION

The Cretaceous-Paleogene boundary (KPB) is one of the best-documented intervals in Earth's history and yet remains a subject of intensive research (Hull et al., 2020). Episodes of global climatic change during the ~1 m.y. across the KPB include, among others, the Late Maastrichtian Warming Event (LMWE) and the Danian Dan-C2 event. The LMWE is associated with a transient 2°–5° C global warming ~150–300 k.y. prior to the KPB (Woelders et al., 2017), and the Dan-C2 event with a 4° C sea-surface temperature rise ~200–300 k.y. after the KPB (Quillévéré et al., 2008). Recent improvements in radiometric dating ($^{40}Ar/^{39}Ar$ and U-Pb) of Deccan volcanism (Schoene et al., 2019; Sprain et al., 2019) suggest causal links between Deccan activity and climatic perturbations around the KPB (Barnet et al., 2018; Krahl et al., 2020). However, uncertainties in correlation mean that the timing of Deccan volcanism and its climatic effects over the KPB interval are still under intense discussion (e.g., Hull et al., 2020; Keller et al., 2020). Complete and expanded climate-sensitive archives with detailed age control are crucial to provide new insights into this classic problem.

The Zumaia outcrop in northwestern Spain (Fig. 1) is an auxiliary section for the Global Boundary Stratotype Section and Point (GSSP) for the base of the Danian (Molina et al., 2009). The KPB at Zumaia is marked by an altered microtektite-rich airfall layer overlain by a 9-cm-thick blackish clay bed, which together form the KPB clay (Figs. S1B–S1E in the Supplemental Material[1]), separating the rhythmic marl-limestone alternations of Maastrichtian and Danian ages. The exceptional and cyclic exposure of the Zumaia outcrop (Fig. S1A) forms the basis of cyclostratigraphic age models (e.g., Batenburg et al. [2012] for the Maastrichtian, and Dinarès-Turell et al. [2014] for the Paleocene). We present integrated Maastrichtian and Danian astrochronologies over a 1-m.y.-long interval, providing ages for paleobiological and paleoclimate events identified in new high-resolution micropaleontological, geochemical, and geophysical data. Detailed age control of episodes of climate change during the KPB interval, i.e., the LMWE, Dan-C2, and the Lower C29n (LC29n) events, allows us to test to what degree Deccan volcanism and orbital forcing contributed to environmental change.

METHODS AND AGE MODEL

We collected 171 rock samples in the 24.5-m-thick interval across the KPB at Zumaia for micropaleontological, geochemical, and geophysical analyses. Carbon isotope ($\delta^{13}C$), calcium carbonate ($CaCO_3$), magnetic susceptibility (χ), and foraminiferal analyses followed standard procedures. $\delta^{13}C$ data were calibrated to the in-house NOCZ Carrara marble standard, showing analytical precision better than $\pm 1\sigma$ (<0.1‰ Vienna Peedee belemnite [VPDB]). See Text S1 in the Supplemental Material for detailed methods.

Our age model was constructed by correlating to the stable 405 k.y. component of long

[1]Supplemental Material. Text S1 (detailed methodology), Text S2 (geochemical and geophysical properties), Text S3 (detailed age models), Text S4 (further evidence of the stratigraphic continuity across the KPB at Zumaia), Tables S1–S5, and Figures S1–S5. Please visit https://doi.org/10.1130/GEOL.S.15152583 to access the supplemental material, and contact editing@geosociety.org with any questions.

CITATION: Gilabert, V., et al., 2021, Contribution of orbital forcing and Deccan volcanism to global climatic and biotic changes across the Cretaceous-Paleogene boundary at Zumaia, Spain: Geology, v. 50, p. 21–25, https://doi.org/10.1130/G49214.1

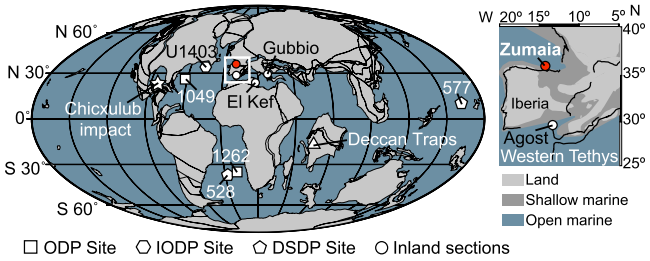

Figure 1. Paleogeographic reconstruction for the Cretaceous-Paleogene boundary (66 Ma), with localities cited in this study (after https://www.odsn.de/odsn/services/paleomap/adv_map.html). ODP—Ocean Drilling Program; IODP—International Ocean Discovery Program; DSDP—Deep Sea Drilling Project.

eccentricity-modulated precession as identified by Batenburg et al. (2012) and Dinarès-Turell et al. (2014). The tie points for age calibration were the 405 k.y. maxima and minima extracted from the La2011 astronomical solution (Laskar et al., 2011) and a KPB age of 66.001 Ma (Dinarès-Turell et al., 2014). This age for the KPB differs from those of recent U-Pb and $^{40}Ar/^{39}Ar$ dating efforts, which yielded results of 66.016 ± 0.05 Ma (Schoene et al., 2019) and 66.052 ± 0.008/0.043 Ma (Sprain et al., 2018), respectively, but falls within the uncertainties of these estimates. The stratigraphic position of the tie points is shown in Figure 2 and listed with ages in Table S1 in the Supplemental Material. We assume that each limestone-marlstone couplet represents a precession cycle, and the $CaCO_3$ (%) and χ (m^3/kg) data support the identification of lithological alternations (Table S2; Fig. S2). Based on cosmic ^{3}He sedimentation rates, the KPB clay spans the first ~10 k.y. of the Danian (Mukhopadhyay et al., 2001), approximately half of a precession cycle. According to the 405 k.y. cyclostratigraphic framework of Dinarès-Turell et al. (2014), the interval between the KPB and the first Danian eccentricity minimum (~50 cm above the KPB) spans 34 k.y., which is compatible with the 1.5 precession cycles estimated here (Fig. 2). Calibrated ages assigned to each sample were linearly interpolated within each precession cycle between the tie points. This method has allowed us to account for large, orbitally driven changes in sedimentation rate in the Zumaia section, providing a detailed age calibration of the recognized paleobiological and paleoclimatic events in the 1 m.y. across the KPB (Table S2). Detailed methods, age model data, and stratigraphy are provided in Texts S1–S4.

RESULTS

Calibration of Planktic Foraminiferal Events

At Zumaia, the lowest occurrence datum (LOD) of *Plummerita hantkeninoides*, the index species of Biozone CF1, is at −4.55 m (Fig. 2; Fig. S3; Table S3), i.e., 99 k.y. prior to the KPB. After intensive study, we recognized the LODs of the index species *Parvularugoglobigerina longiapertura*, *P. eugubina*, *Eoglobigerina simplicissima*, *Parasubbotina pseudobulloides*, *Subbotina triloculinoides*, and *Globanomalina compressa* at 6, 23, 37, 100, 330, and 655 cm above the KPB, respectively (Fig. 2; Fig. S3; Table S4); i.e., 7, 18, 26, 68, 210, and 473 k.y. after the KPB, respectively. These datums mark the bases of the lower Danian biozones of Arenillas et al. (2004). Their equivalence with biozones P0, Pα, P1a, P1b, and P1c of Wade et al. (2011) is shown in Figure 2.

The planktic foraminiferal assemblages remained relatively stable at Zumaia during the last ~400 k.y. of the late Maastrichtian (Fig. S4), with only a minor and transient assemblage reorganization related to an increase in *Heterohelix* abundance (~50% to 65%–80%) from 11 to 7.5 m below the KPB (~250–150 k.y. prior to the KPB). Conversely, the lower Danian oligotaxic assemblages are characterized by a rapid succession of planktic foraminiferal acme stages (PFAS of Arenillas et al., 2006) and blooms of opportunistic nannoplankton taxa (e.g., *Thoracosphaera*, *Braarudosphaera*, and *Neobiscutum*) (Bernaola et al., 2006, Table S2). We recognized PFAS-1 (acme of triserial *Guembelitria*) from the KPB up to 6 cm; PFAS-2 (acme of tiny trochospiral *Parvularugoglobigerina* and *Palaeoglobigerina*) from 6 to 55 cm; and PFAS-3 (acme of biserial *Woodringina* and *Chiloguembelina*) from 55 cm upward. A second bloom of triserial guembelitriids (*Chiloguembelitria*) is recognized in PFAS-3 from 195 to 400 cm (Table S4). According to our age model, the bases of the three main PFASs (1, 2, and 3) are calibrated to 0, 7, and 42 k.y. after the KPB, respectively, and the *Chiloguembelitria* bloom to 110 to 282 k.y.

Calibration of Carbon Isotope Excursions (CIEs)

In the upper Maastrichtian of Zumaia, the main decrease in $\delta^{13}C$ is recorded between 11.05 and 4.75 m (~250 and 100 k.y.) below the KPB, showing a distinctive gradual shift to the lowest $\delta^{13}C$ values of the studied section, except for those reached at the KPB (Fig. 3C). From 55 cm (42 k.y.) above the KPB upward, $\delta^{13}C$ shows an overall trend to lower isotopic values, interrupted by two distinctive negative CIEs (Fig. 3C). The first, with the shape of a double spike, is recorded between 3.15 and 4.30 m (~200 and 305 k.y.) above the KPB, and the second between 7.1 and 7.9 m (~520 and 595 k.y.). We suggest that these isotopic events recognized at Zumaia correspond to the LMWE, Dan-C2, and LC29n events reported at Gubbio, Italy (Tethys; Coccioni et al., 2010; Voigt et al., 2012), Ocean Drilling Program (ODP) Site 1049 and International Ocean Discovery Program (IODP) Site U1403 (North Atlantic; Quillévéré et al., 2008; Batenburg et al., 2018), and ODP Site 1262 (South Atlantic; Woelders et al., 2017), confirming the global character of these carbon-cycle perturbations (Figs. 1 and 3).

DISCUSSION AND CONCLUSION

To investigate the potential impact of volcanism, we focus on changes in carbon-cycle and climatic events before and after the KPB boundary, excluding the Chicxulub asteroid–induced KPB event. The astronomically calibrated $\delta^{13}C$ record of Zumaia is compared in Figure 3 to those of other reference sites and sections from the Atlantic and Tethys Oceans and to the main period of Deccan Traps eruptions according to the models of Schoene et al. (2019) and Sprain et al. (2019). The LMWE, calibrated here to an age of 66.25–66.10 Ma, coincides with a minor eruptive phase of the Deccan Traps (Kalsubai and Lonavala subgroups) in both eruptive models (Fig. 3B). Recent carbon and CO_2 estimations from Deccan outgassing suggest that this phase could have outgassed more CO_2 than the main eruptive phases of the Wai subgroup, but this would still have been insufficient to explain the amplitude of LMWE warming (Hernandez Nava et al., 2021). However, both warming (Hull et al., 2020; Fig. 3D) and carbon-cycle changes follow the rhythm of long eccentricity (405 k.y. periodicity). The peak perturbation of the LMWE occurs at the eccentricity maximum $Ma_{405}1$ (Figs. 3A and 3C), rather than preceding it as suggested by Barnet et al. (2018), coinciding with increased amplitudes of orbital forcing and seasonality. We hypothesize that raised CO_2 levels through Deccan outgassing during the late Maastrichtian may have amplified climate sensitivity to orbital forcing, resulting in the enhanced global climatic response of the LMWE. Similarly, late Paleocene–early Eocene hyperthermals have been linked to 405 k.y. eccentricity maxima during the emplacement of the North Atlantic igneous province (Barnet et al., 2019).

From the LMWE to the KPB, a gradual cooling is recognized worldwide (Woelders et al., 2017; Barnet et al., 2018; Hull et al., 2020). This pre-KPB cooling did not cause substantial changes in the foraminiferal assemblages of Zumaia, except for the extinction of *Archaeoglobigerina cretacea* (Fig. 2; Fig. S3). This points to planktic foraminiferal evolutionary and environmental stability during the latest Maastrichtian, as previously suggested (Gilabert et al., 2021a, and references therein). At

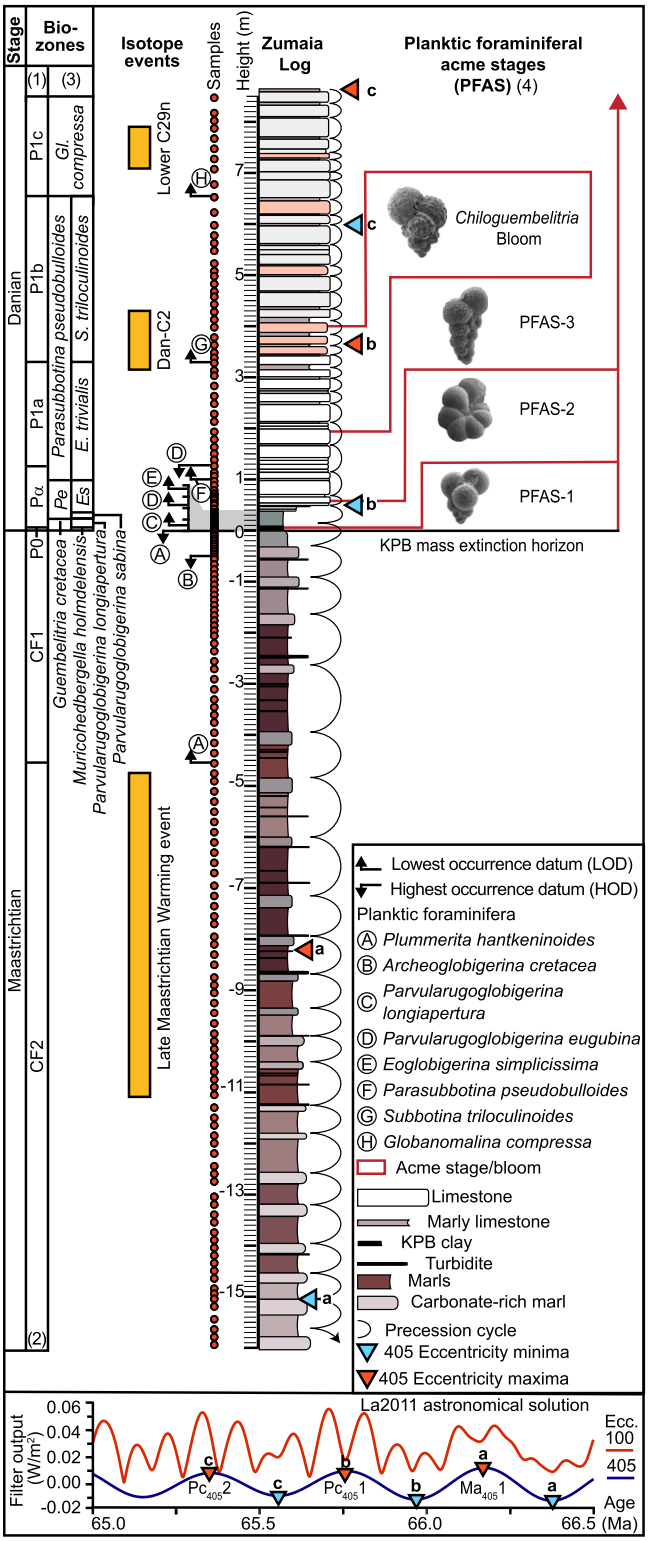

Figure 2. Stratigraphic log for planktic foraminiferal datums, biozones, and isotopic events recognized at Zumaia (Spain). Stratigraphic positions of 405 k.y. tie points (colored triangles) are based on the La2011 astronomical solution (Laskar et al., 2011). $Pc_{405}2$, $Pc_{405}1$—Paleocene eccentricity maxima 1 and 2; $Ma_{405}1$—Maastrichtian eccentricity maximum 1. Biozonations: (1)—Wade et al. (2011); (2)—Li and Keller (1998); (3)—Arenillas et al. (2004). (4)—planktic foraminiferal acme stages (PFAS) of Arenillas et al. (2006). *Gl.*—*Globanomalina*; *S.*—*Subbotina*; *E.*—*Eoglobigerina*; *Es*—*Eoglobigerina simplicissima*; *Pe*—*Parvularugoglobigerina eugubina*; KPB—Cretaceous-Paleogene boundary; Ecc.—eccentricity (in k.y.).

Zumaia, an absence of pre-KPB perturbations in the global carbon cycle is also observed, which calls into question the hypothesis by Schoene et al. (2019) and Keller et al. (2020) of a Deccan eruptive megapulse in the late Maastrichtian, associated with the emplacement of the Poladpur Formation (Fig. 3).

After the KPB, the first carbon cycle perturbation in the Paleocene is the Dan-C2 event (dated here at 65.8–65.7 Ma), which is characterized by two distinctive CIEs according to bulk and calcareous plankton $\delta^{13}C$ data (Quillévéré et al., 2008). Whether the Dan-C2 event represents a true hyperthermal is debated due to the absence of bottom-water warming (Barnet et al., 2019). The Dan-C2 event is closely aligned with two short eccentricity maxima within the long eccentricity maximum $Pc_{405}1$ (Figs. 3A and 3C), suggesting strong orbital control (Quillévéré et al., 2008; Sinnesael et al., 2019). However, the extrusion of the lava flows of the Ambenali Formation has also been considered a possible trigger for the Dan-C2 event (Krahl et al., 2020). Our astronomically calibrated age model does not reveal a direct temporal link between the Dan-C2 event and the Ambenali Formation (Fig. 3B) using either the model of isolated megapulses of Schoene et al. (2019) or the quasi-continuous model of Sprain et al. (2019), the latter recalculated in terms of eruptive rate by Schoene et al. (2021) (Fig. 3B). According to Sprain et al. (2019), the Ambenali Formation was emplaced over a much longer period (~350 k.y.) than the duration of the Dan-C2 event (~100 k.y.), beginning long before it and ending long after it, and thus refuting a direct cause-effect relationship. According to Schoene et al. (2019), the Ambenali Formation was emplaced during a volcanic megapulse well before the beginning of the Dan-C2 event, suggesting seemingly unlinked events. In addition, Hull et al. (2020) and Fendley et al. (2020) have recently proposed that Deccan volcanic outgassing alone was insufficient to significantly alter early Danian climate. By contrast, a combination of both orbital forcing and an overall increase in atmospheric CO_2 associated with Ambenali Formation emplacement could have caused the carbon cycle to briefly cross a critical threshold for carbon release twice, resulting in the double-peak CIE of the Dan-C2 event. Double-peak CIEs characterize several Paleogene hyperthermals (Coccioni et al., 2012) and have been related to extreme orbital configurations separated by an interlude of rapid replenishment (<100 k.y.) of carbon reservoirs (Barnet et al., 2019).

Finally, the LC29n event (65.48–65.41 Ma) seems to be minor, is not reported worldwide, and is not accompanied by relevant paleoenvironmental and paleobiological changes. Nevertheless, it coincides with a short eccentricity maximum (Figs. 3A and 3C) and possibly with the final stages of Deccan volcanism according to the model of Sprain et al. (2019).

According to our data, unlike the Dan-C2 and LC29n events, the onset of the bloom of eutrophic and/or opportunistic *Chiloguembelitria* (commonly assigned to the genus *Guembelitria*) is consistently coeval with the onset of Ambenali Formation emplacement at ca. 65.9 Ma (Figs. 3A and 3B). This bloom has been recognized at Zumaia and other open-ocean sites worldwide (Fig. S5), such as Deep Sea Drilling Project (DSDP) Site 577 (central Pacific; Smit and Romein, 1985), Agost (Spain; Canudo et al., 1991), ODP Site 528 (South Atlantic; D'Hondt and Keller, 1991), Gubbio (Italy; Coccioni et al., 2010), El Kef (Tunisia; Arenillas et al., 2018), and Caravaca (Spain; Gilabert et al., 2021b).

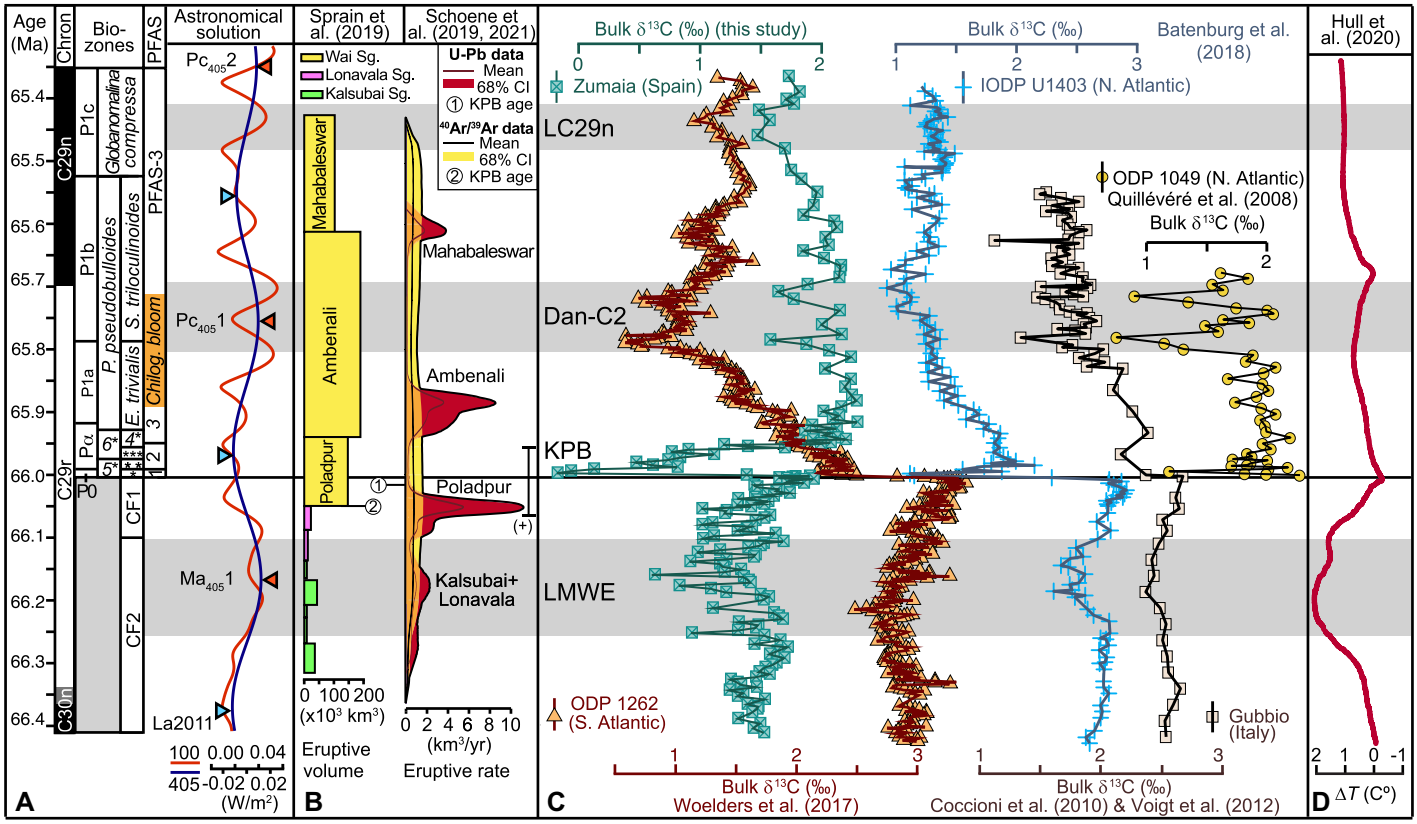

Figure 3. Temporal correlation of planktic foraminiferal biozones and acme stages (PFAS) with the La2011 astronomical solution (Laskar et al., 2011) (A), Deccan eruptive models (B), bulk δ^{13}C curves in several open-ocean localities on independent age models (C), and global temperature change across Cretaceous-Paleogene boundary (KPB) (D). Chron C29r-C30n and C29r-C29n reversals are based, respectively, on Batenburg et al. (2012) and Dinarès-Turell et al. (2014). *—*Muricohedbergella holmdelensis*; **—*Parvularugoglobigerina longiapertura*; *—*Parvularugoglobigerina sabina*; 4*—*Eoglobigerina simplicissima*; 5*—*Guembelitria cretacea*; 6*—*Parvularugoglobigerina eugubina*; *E.*—*Eoglobigerina*; *S.*—*Subbotina*; *P.*—*Parasubbotina*; *Chilog.*—*Chiloguembelitria*; Sg.—subgroup; colored triangles—405 k.y. eccentricity tie points; Pc$_{405}$2, Pc$_{405}$1—Paleocene eccentricity maxima 1 and 2; Ma$_{405}$1—Maastrichtian eccentricity maximum 1; LMWE—late Maastrichtian warming event; Δ*T*—temperature variation; (+)—uncertainty range for KPB within Deccan Traps, taken from Schoene et al. (2021); CI—confidence interval.**

We hypothesize that the massive input of nutrients to the surface ocean due to effusive Deccan volcanism may have been a stressor for pelagic ecosystems starting ~90 k.y. before the Dan-C2 event. The residence time of nutrients in the surface ocean may have been longer in the Danian due to the reduction in the efficiency of the biological pump (Birch et al., 2016), which could have allowed for a worldwide proliferation of opportunistic taxa in the open ocean for longer time intervals. Nonetheless, the absence of global changes in temperature and the carbon cycle prior to the Dan-C2 event suggests that orbital forcing was required to exacerbate the effect of long-term CO_2 emissions of Deccan volcanism during the Dan-C2 event. Our integrated stratigraphic results from Zumaia thus explain why the eruptive events of the Deccan Traps left a pronounced climatic signature only when they coincided with times of enhanced orbital forcing.

ACKNOWLEDGMENTS

We thank A. Gale and two anonymous reviewers for their constructive reviews. This work was supported by the Ministerio de Ciencia, Innovación y Universidades (MCIU) / Agencia Estatal de Investigación (AEI) / Fondo Europeo de Desarrollo Regional (FEDER) (grant PGC2018-093890-B-I00), and by the Aragonese Government/FEDER (grant DGA group E33_20R). V. Gilabert is supported by the Spanish Ministry of Economy and Competitiveness (MINECO) (FPI grant BES-2016-077800). We thank S.A. Robinson, A. Hilario, J.C. Larrasoaña, and the Basque Coast UNESCO Global Geopark for support, and R. Glasgow for improving the English text. This research is part of the Ph.D. thesis of V. Gilabert.

REFERENCES CITED

Arenillas, I., Arz, J.A., and Molina, E., 2004, A new high-resolution planktic foraminiferal zonation and subzonation for the lower Danian: Lethaia, v. 37, p. 79–95, https://doi.org/10.1080/00241160310005097.

Arenillas, I., Arz, J.A., Grajales-Nishimura, J.M., Murillo-Muñetón, G., Alvarez, W., Camargo-Zanoguera, A., Molina, E., and Rosales-Domínguez, C., 2006, Chicxulub impact event is Cretaceous/Paleogene boundary in age: New micropaleontological evidence: Earth and Planetary Science Letters, v. 249, p. 241–257, https://doi.org/10.1016/j.epsl.2006.07.020.

Arenillas, I., Arz, J.A., and Gilabert, V., 2018, Blooms of aberrant planktic foraminifera across the K/Pg boundary in the Western Tethys: Causes and evolutionary implications: Paleobiology, v. 44, p. 460–489, https://doi.org/10.1017/pab.2018.16.

Barnet, J.S.K., Littler, K., Kroon, D., Leng, M.J., Westerhold, T., Röhl, U., and Zachos, J.C., 2018, A new high-resolution chronology for the late Maastrichtian warming event: Establishing robust temporal links with the onset of Deccan volcanism: Geology, v. 46, p. 147–150, https://doi.org/10.1130/G39771.1.

Barnet, J.S.K., Littler, K., Westerhold, T., Kroon, D., Leng, M.J., Bailey, I., Röhl, U., and Zachos, J.C., 2019, A high-fidelity benthic stable isotope record of late Cretaceous–early Eocene climate change and carbon-cycling: Paleoceanography and Paleoclimatology, v. 34, p. 672–691, https://doi.org/10.1029/2019PA003556.

Batenburg, S.J., et al., 2012, Cyclostratigraphy and astronomical tuning of the Late Maastrichtian at Zumaia (Basque country, Northern Spain): Earth and Planetary Science Letters, v. 359–360, p. 264–278, https://doi.org/10.1016/j.epsl.2012.09.054.

Batenburg, S.J., et al., 2018, Late Maastrichtian carbon isotope stratigraphy and cyclostratigraphy of the Newfoundland Margin (Site U1403, IODP Leg 342): Newsletters on Stratigraphy, v. 51, p. 245–260, https://doi.org/10.1127/nos/2017/0398.

Bernaola, G., Baceta, J.I., Payros, A., Orue-Etxebarria, X., and Apellaniz, E., eds., 2006, The Paleocene and lower Eocene of the Zumaia section (Basque Basin): Climate and Biota of the Early Paleo-

gene 2006, Post Conference Field Trip Guidebook: Bilbao, Spain, University of the Basque Country, 82 p.

Birch, H.S., Coxall, H.K., Pearson, P.N., Kroon, D., and Schmidt, D.N., 2016, Partial collapse of the marine carbon pump after the Cretaceous-Paleogene boundary: Geology, v. 44, p. 287–290, https://doi.org/10.1130/G37581.1.

Canudo, J.I., Keller, G., and Molina, E., 1991, Cretaceous/Tertiary boundary extinction pattern and faunal turnover at Agost and Caravaca, S.E. Spain: Marine Micropaleontology, v. 17, p. 319–341, https://doi.org/10.1016/0377-8398(91)90019-3.

Coccioni, R., Frontalini, F., Bancalà, G., Fornaciari, E., Jovane, L., and Sprovieri, M., 2010, The Dan-C2 hyperthermal event at Gubbio (Italy): Global implications, environmental effects, and cause(s): Earth and Planetary Science Letters, v. 297, p. 298–305, https://doi.org/10.1016/j.epsl.2010.06.031.

Coccioni, R., Bancalà, G., Catanzarit, R., Fornaciari, E., Frontalini, F., Giusberti, L., Jovane, L., Luciani, V., Savian, J., and Sprovieri, M., 2012, An integrated stratigraphic record of the Palaeocene–lower Eocene at Gubbio (Italy): New insights into the early Palaeogene hyperthermals and carbon isotope excursions: Terra Nova, v. 24, p. 380–386, https://doi.org/10.1111/j.1365-3121.2012.01076.x.

D'Hondt, S., and Keller, G., 1991, Some patterns of planktic foraminiferal assemblage turnover at the Cretaceous-Tertiary boundary: Marine Micropaleontology, v. 17, p. 77–118, https://doi.org/10.1016/0377-8398(91)90024-Z.

Dinarès-Turell, J., Westerhold, T., Pujalte, V., Röhl, U., and Kroon, D., 2014, Astronomical calibration of the Danian stage (Early Paleocene) revisited: Settling chronologies of sedimentary records across the Atlantic and Pacific Oceans: Earth and Planetary Science Letters, v. 405, p. 119–131, https://doi.org/10.1016/j.epsl.2014.08.027.

Fendley, I.M., et al., 2020, No Cretaceous-Paleogene boundary in exposed Rajahmundry Traps: A refined chronology of the longest Deccan lava flows from $^{40}Ar/^{39}Ar$ dates, magnetostratigraphy, and biostratigraphy: Geochemistry Geophysics Geosystems, v. 21, e2020GC009149, https://doi.org/10.1029/2020GC009149.

Gilabert, V., Arz, J.A., Arenillas, I., Robinson, S.A., and Ferrer, D., 2021a, Influence of the Latest Maastrichtian Warming Event on planktic foraminiferal assemblages and ocean carbonate saturation at Caravaca, Spain: Cretaceous Research, v. 125, 104844, https://doi.org/10.1016/j.cretres.2021.104844.

Gilabert, V., Arenillas, I., Arz, J.A., Batenburg, S.J., and Robinson, S.A., 2021b, Multiproxy analysis of paleoenvironmental, paleoclimatic and paleoceanographic changes during the early Danian in the Caravaca section (Spain): Palaeogeography, Palaeoclimatology, Palaeoecology, v. 576, 110513, https://doi.org/10.1016/j.palaeo.2021.110513.

Hernandez Nava, A., Black, B.A., Gibson, S.A., Bodnar, R.J., Renne, P.R., and Vanderkluysen, L., 2021, Reconciling early Deccan Traps CO_2 outgassing and pre-KPB global climate: Proceedings of the National Academy of Sciences of the United States of America, v. 118, e2007797118, https://doi.org/10.1073/pnas.2007797118.

Hull, P.M., et al., 2020, On impact and volcanism across the Cretaceous-Paleogene boundary: Science, v. 367, p. 266–272, https://doi.org/10.1126/science.aay5055.

Keller, G., et al., 2020, Mercury linked to Deccan Traps volcanism, climate change and the end-Cretaceous mass extinction: Global and Planetary Change, v. 194, 103312, https://doi.org/10.1016/j.gloplacha.2020.103312.

Krahl, G., Bom, M.H.H., Kochhann, K.G.D., Souza, L.V., Savian, J.F., and Fauth, G., 2020, Environmental changes occurred during the Early Danian at the Rio Grande Rise, South Atlantic Ocean: Global and Planetary Change, v. 191, 103197, https://doi.org/10.1016/j.gloplacha.2020.103197.

Laskar, J., Gastineau, M., Delisle, J.-B., Farrés, A., and Fienga, A., 2011, Strong chaos induced by close encounters with Ceres and Vesta: Astronomy and Astrophysics, v. 532, L4, https://doi.org/10.1051/0004-6361/201117504.

Li, L., and Keller, G., 1998, Maastrichtian climate, productivity and faunal turnovers in planktic foraminifera in South Atlantic DSDP sites 525A and 21: Marine Micropaleontology, v. 33, p. 55–86, https://doi.org/10.1016/S0377-8398(97)00027-3.

Molina, E., Alegret, L., Arenillas, I., Arz, J.A., Gallala, N., Grajales-Nishimura, J.M., Murillo-Muñetón, G., and Zaghbib-Turki, D., 2009, The Global Boundary Stratotype Section and Point for the base of the Danian Stage (Paleocene, Paleogene, "Tertiary", Cenozoic): Auxiliary sections and correlation: Episodes, v. 32, p. 84–95, https://doi.org/10.18814/epiiugs/2009/v32i2/002.

Mukhopadhyay, S., Farley, K.A., and Montanari, A., 2001, A short duration of the Cretaceous-Tertiary boundary event: Evidence from extraterrestrial helium-3: Science, v. 291, p. 1952–1955, https://doi.org/10.1126/science.291.5510.1952.

Quillévéré, F., Norris, R.D., Kroon, D., and Wilson, P.A., 2008, Transient ocean warming and shifts in carbon reservoirs during the early Danian: Earth and Planetary Science Letters, v. 265, p. 600–615, https://doi.org/10.1016/j.epsl.2007.10.040.

Schoene, B., Eddy, M.P., Samperton, K.M., Keller, C.B., Keller, G., Adatte, T., and Khadri, S.F.R., 2019, U-Pb constraints on pulsed eruption of the Deccan Traps across the end-Cretaceous mass extinction: Science, v. 363, p. 862–866, https://doi.org/10.1126/science.aau2422.

Schoene, B., Eddy, M.P., Keller, C.B., and Samperton, K.M., 2021, An evaluation of Deccan Traps eruption rates using geochronologic data: Geochronology, v. 3, p. 181–198, https://doi.org/10.5194/gchron-3-181-2021.

Sinnesael, M., et al., 2019, Multiproxy Cretaceous-Paleogene boundary event stratigraphy: An Umbria-Marche basinwide perspective, *in* Koeberl, C. and Bice, D.M., eds., 250 Million Years of Earth History in Central Italy: Celebrating 25 Years of the Geological Observatory of Coldigioco: Geological Society of America Special Paper 542, p. 133–158, https://doi.org/10.1130/2019.2542(07).

Smit, J., and Romein, A.J.T., 1985, A sequence of events across the Cretaceous-Tertiary boundary: Earth and Planetary Science Letters, v. 74, p. 155–170, https://doi.org/10.1016/0012-821X(85)90019-6.

Sprain, C.J., Renne, P.R., Clemens, W.A., and Wilson, G.P., 2018, Calibration of chron C29r: New high-precision geochronologic and paleomagnetic constraints from the Hell Creek region, Montana: Geological Society of America Bulletin, v. 130, p. 1615–1644, https://doi.org/10.1130/B31890.1.

Sprain, C.J., Renne, P.R., Vanderkluysen, L., Pande, K., Self, S., and Mittal, T., 2019, The eruptive tempo of Deccan volcanism in relation to the Cretaceous-Paleogene boundary: Science, v. 363, p. 866–870, https://doi.org/10.1126/science.aav1446.

Voigt, S., Gale, A.S., Jung, C., and Jenkyns, H.C., 2012, Global correlation of upper Campanian–Maastrichtian successions using carbon-isotope stratigraphy: Development of a new Maastrichtian timescale: Newsletters on Stratigraphy, v. 45, p. 25–53, https://doi.org/10.1127/0078-0421/2012/0016.

Wade, B.S., Pearson, P.N., Berggren, W.A., and Pälike, H., 2011, Review and revision of Cenozoic tropical planktonic foraminiferal biostratigraphy and calibration to the geomagnetic polarity and astronomical time scale: Earth-Science Reviews, v. 104, p. 111–142, https://doi.org/10.1016/j.earscirev.2010.09.003.

Woelders, L., et al., 2017, Latest Cretaceous climatic and environmental change in the South Atlantic region: Paleoceanography, v. 32, p. 466–483, https://doi.org/10.1002/2016PA003007.

Printed in USA